Sepehr, Amir; Pouresmaeil, Mobina; Pouresmaeil, Edris

Harmonic Stability Analysis of Grid-Connected Converters with Power Synchronization Control

Published in:
2021 IEEE PES Innovative Smart Grid Technologies Europe (ISGT-Europe)

DOI:
10.1109/ISGTEurope52324.2021.9640199

Published: 01/01/2021

Document Version
Peer-reviewed accepted author manuscript, also known as Final accepted manuscript or Post-print

Harmonic Stability Analysis of Grid-Connected Converters with Power Synchronization Control

Amir Sepehr
Dept. of Elec. Eng. and Automation
Aalto University
Espoo, Finland
amir.sepehr@aalto.fi

Mobina Pouresmaeil
Dept. of Elec. Eng. and Automation
Aalto University
Espoo, Finland
mobina.pouresmaeil@aalto.fi

Edris Pouresmaeil
Dept. of Elec. Eng. and Automation
Aalto University
Espoo, Finland
edris.pouresmaeil@aalto.fi

***Abstract*—Integration of power electronic-based renewable energy sources into weak grids brings new concerns regarding the harmonic stability of modern power systems. This paper studies harmonic stability and impedance characteristics of power synchronization control (PSC) which has been introduced for control of converters under weak grid operating condition. Due to the varying grid impedance in weak grids, the harmonic stability of converters with LCL output filters would be a demanding prospect. Thus, this paper addresses this issue by studying the admittance characteristics of PSC based on the dynamics of the control scheme, the delay and the sampling frequency of the control system, and the linearized model of the grid-connected converter. Finally, the critical grid inductance and the sufficient conditions for achieving harmonic stability are introduced. Time-domain simulations are carried out to support the proposed harmonic stability analysis.**

Keywords—harmonic stability, LCL filter, output impedance, power synchronization control, weak grid

I. INTRODUCTION

Moving towards a sustainable society has commercialized the integration of renewable energy sources into power systems. Widely used power electronic converters are the foremost interfaces between renewable energy sources and the power grid [1]. The demand for renewable energy generation in remote points with high impedance grids in addition to the high number of power electronic converters connected to the modern power grid, poses new challenges regarding the harmonic stability and power quality of the power system [2], [3].

Although every individual converter's control system is programmed and designed for stable operation in accordance with the grid condition, the power quality and harmonic stability at the connection point of each converter would be jeopardized under weak grid operating condition due to the interaction between the varying impedance of the grid, the delay and the sampling frequency of the control system, and the dynamics of the control scheme [1]-[4]. Interaction between the converter output impedance and the varying grid impedance may result in undamped resonances in the output LCL filter of the converter [4]. Recent research works exhibit that the delay and the sampling frequency of the control system coupled with the converter control scheme and the converter output filter parameters adversely affect the damping characteristics of the power electronic converters [1], [2]. Mitigation of the undamped resonances can be achieved by studying and analyzing the output impedance and damping characteristics of the converters.

Furthermore, in power electronics dominated power systems, the emulation of synchronous machine dynamics by power converters has become an evolving concept [5]. Synchronous machines provide synchronizing torque, damping, and inertia as the main ancillary support during disturbances in power systems [5]. Accordingly, various control schemes based on synchronous machine principles have been developed for weak grid applications. In this respect, power synchronization control scheme (PSCS), which is a voltage-stiff control scheme, has been proposed to emulate the dynamic response and features of synchronous machines with robust control on voltage and frequency to deal with the dynamic issues of weak grids [5], [6]. Particularly, PSCS represents a viable solution that allows transferring power between remote points of the grid and demonstrates technical advantages in high-impedance-grid applications [6]. However, the harmonic stability and the output impedance characteristics of PSCS have not been studied over a wide frequency range in literature.

The interaction between the converter control system and the LCL filter may cause undamped resonances in a wide range of frequency. The broad system harmonic stability can be studied by modelling the output impedance of the converter in a wide frequency range. If the converter output impedance has a phase angle in the interval of $[-\pi/2, \pi/2]$, the potential resonances would be damped inherently, otherwise a particular selection of sampling frequency, active damping, passive damping, and LCL filter parameters is required. In practice, the time delay of the converter control system may result in harmonic instability under certain grid impedances [2], [7]. Therefore, employing an appropriate damping technique is needed to guarantee the stable operation of the converter. Since the passive damping techniques impose extra power dissipation and inferior efficiency, employing active damping techniques has gained increasing attention. However, the time delay of the converter control system including sampling, computation, and modulation introduce a critical frequency which is one-sixth of the sampling frequency of the converter [7]. Under weak grid condition where the grid impedance has a varying characteristic, this time delay implies that the active damping may fail to mitigate the undamped resonances in specific frequency ranges. Thus, the output impedance of the converter should be modelled by considering the dynamics of the control scheme, the delay and the sampling frequency of the control system, and the linearized model of the grid-connected converter.

Therefore, this paper aims to address the harmonic stability of PSCS-based converters by studying and analyzing the output impedance characteristics of the converter over a wide frequency range.

The rest of this paper is organized as follows: Section II explains the principles of PSCS for grid-connected converters. Section III presents modelling the dynamics of the converter control system over a wide frequency range. Section IV discusses the non-passive range of the converter output admittance and presents the harmonic stability analysis for various grid impedances. Time-domain simulations are presented in Section V to verify the proposed harmonic stability analysis. Finally, Section VI summarizes and highlights the main conclusions of this paper.

II. Principles and Dynamics of PSCS

The general diagram of a PSCS-based grid-connected converter is depicted in Fig. 1, where control scheme is founded on the active power synchronization. The angle of the voltage reference of the converter is generated by the active power error that is defined as the difference between the converter output active-power and the reference of the active-power. In PSCS, converter synchronization with the grid is inspired by the synchronization mechanism of a synchronous generator. The description of PSCS for a grid-connected voltage-source converter is presented in detail in [8], and [3]. In PSCS, the active power control and synchronization with the ac system are performed through power synchronization loop (PSL) given by

$$\delta = K_{ip}\int (P_{ref} - P_g) \tag{1}$$

$$\theta = K_{ip}\int (P_{ref} - P_g) + \omega_0 t \tag{2}$$

where δ is the power angle which denotes the phase difference between the converter voltage and the grid voltage. θ and K_{ip} are the generated phase angle and the integral gain of PSL, respectively. P_{ref} is the active power reference, P_g is the measured output active power at the point of connection, and ω_0 denotes the grid frequency. In order to provide damping against potential resonances, converter voltage-reference vector $\mathbf{v}_{ref}^{dq}$ in synchronous reference frame (SRF) is generated by the voltage-vector control law expressed by

$$\begin{aligned} \mathbf{v}_{ref}^{dq} &= V_0 - H(s)\mathbf{i}^{dq} \\ H(s) &= \frac{R_d s}{s+\omega_b} \end{aligned} \tag{3}$$

where, V_0 is the nominal voltage, $\mathbf{i}^{dq}$ is the converter current vector in SRF, and $H(s)$ is a high-pass filter for obtaining damping in which R_d and ω_b are the gain and bandwidth of the high-pass filter, respectively. Also, a backup PLL is embedded in the control system for smoothing initial synchronization with the grid and generates the $\omega_0 t$ term [3]. The vector of the converter voltage $\mathbf{v}_{ref}^{\alpha\beta}$ in the stationary-reference frame $\alpha\beta$ can be expressed by

$$\mathbf{v}_{ref}^{\alpha\beta} = \mathbf{v}_{ref}^{dq} e^{j\theta} \tag{4}$$

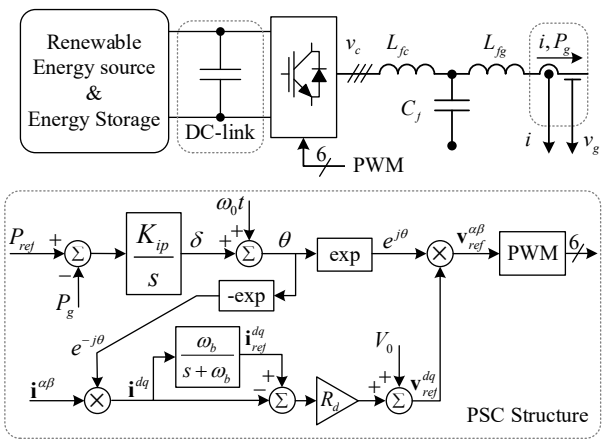

Fig. 1. General diagram of a PSCS-based grid-connected converter with LCL filter and the control system.

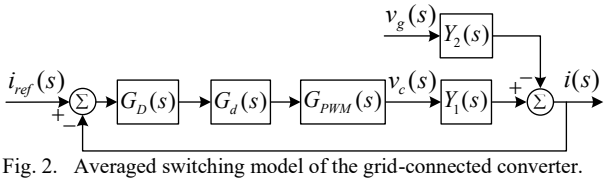

Fig. 2. Averaged switching model of the grid-connected converter.

In PSCS, $\mathbf{v}_{ref}^{dq}$ and θ are the control variables regulated by the controller to reach the references of the connection point voltage and the output active power, respectively.

III. Output Impedance Modeling of a PSCS-Based Converter Over a Wide Frequency Range

As shown in Fig. 1, PSCS includes a high-pass filter with a virtual resistance which can be modelled as a current controller $G_D(s)$ for proving damping of high-order current components. In addition, a time delay $G_d(s)$ resulting from the computation and the pulse width modulation (PWM) should be considered to model the internal dynamics of PSCS. Also, the gain of the PWM can be modelled by $G_{PWM}(s)$. Thus, an average switching model as depicted in Fig. 2 can be obtained by defining

$$\begin{aligned} G_D(s) &= R_d \\ G_d(s) &= e^{-1.5T_s s} \\ G_{PWM}(s) &= 1 \end{aligned} \tag{5}$$

where T_s is the sampling time of the converter control system. The LCL filter (as shown in Fig. 1) is modelled by neglecting the resistive parts of the passive elements. Thus, the input-output relations of the LCL filter can be modelled by the two admittances $Y_1(s)$ and $Y_2(s)$ defined as:

$$\begin{aligned} Y_1(s) &= \left.\frac{i_g}{v_c}\right|_{v_{PCC}=0} = \frac{1}{s(s^2 C_f L_{fc} L_{fg} + L_{fc} + L_{fg})} \\ Y_2(s) &= \left.\frac{-i_g}{v_{PCC}}\right|_{v_c=0} = \frac{s^2 C_f L_{fc} + 1}{s(s^2 C_f L_{fc} L_{fg} + L_{fc} + L_{fg})}. \end{aligned} \tag{6}$$

Therefore, the converter output admittance is modelled by $Y_{Conv}(s)$ as:

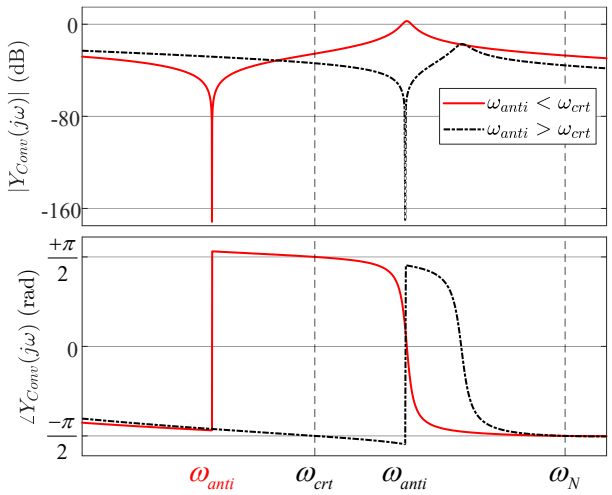

Fig. 3. Bode diagram of the converter output admittance $Y_{Conv}(s)$ for two possible LCL-filter selection ($\omega_{anti} > \omega_{crt}$ and $\omega_{anti} < \omega_{crt}$).

$$Y_{Conv}(s) = \frac{i_g}{v_{PCC}}\bigg|_{i_{ref}=0} = \frac{Y_2}{1+G_c G_d Y_1} = \frac{s^2 C_f L_{fc} + 1}{s^3 C_f L_{fc} L_{fg} + s(L_{fc} + L_{fg}) + R_d e^{-1.5T_s s}}. \quad (7)$$

A. *Harmonic stability analysis by the converter output admittance*

By assuming that the complex admittance network consists of several sub-systems, the harmonic stability of the integrated system depends on the relations between the admittances. Noting that in a stable system with only passive sub-systems, the maximum phase angle of the unified system should be in the $[-\pi, \pi]$, which never encircles $(-1, j0)$ in the Nyquist plot. Thus, by applying the constraint of passivity on every individual grid-connected converter over a wide frequency range, the harmonic stability of the entire system would be achieved for all operating conditions.

Fig. 3 shows the typical bode diagrams of a PSCS-based grid-connected converter with LCL filter for two different possible filter parameter selection. Both of the filter parameter selections bring remarkable variations in the frequency response of the system. For instance, the magnitude of the converter output admittance presents a noticeable dip the anti-resonance frequency ω_{anti} given by

$$\omega_{anti} = \sqrt{C_f L_f}^{-1} \quad (8)$$

which originates from the double zeros of (8). In order to limit the area of the harmonic stability analysis to the relevant frequency range of possible harmonic resonances, three coordinates are defined in the following. The resonance frequency of LCL filter ω_{res} , the critical frequency of the converter ω_{crt} and the Nyquist frequency ω_N given by

$$\omega_{res} = \sqrt{\frac{L_{fc} + L_{fg}}{L_{fc} L_{fg} C_f}}$$
$$\omega_{crt} = \omega_s / 6 \quad (9)$$
$$\omega_N = \omega_s / 2$$

where ω_s is the sampling frequency of the control system (in *rad/sec*). The Nyquist frequency ω_N denotes one half of the sampling frequency of the control system. The critical frequency of the converter ω_{crt} is defined as one-sixth of the sampling frequency. In case $\omega_{res} > \omega_{crt}$, no resonance damping is required for stable operation of the converter in the stand-alone mode.

The value of the anti-resonance frequency ω_{anti} with regard to the critical frequency ω_{crt} , ($\omega_{anti} < \omega_{crt}$ or $\omega_{anti} > \omega_{crt}$) , causes two classifiable cases in respect to the passivity zone of $Y_{Conv}(s)$ as depicted in Fig. 3. Due to the inductive characteristics of the filter, the phase angle of $Y_{Conv}(s)$ starts with 0 and ends with $-\pi/2$ in the both cases. However, the phase angle of $Y_{Conv}(s)$ exceeds the passive range $[-\pi/2, +\pi/2]$ in two different intervals of $(\omega_{anti}, \omega_{crt})$ or $(\omega_{crt}, \omega_{anti})$, respectively. In addition, a phase angle jump occurs due to the time delay introduced by $G_d(s)$. Thus, the time delay and the anti-resonance frequency ω_{anti} represent an integral role in the harmonic stability of the system.

B. *Non-passive zone of the converter output admittance*

The non-passivity zone can be identified by exploring the real part of the converter output admittance. Real part of $Y_{Conv}(j\omega)$ can be expressed by

$$\mathrm{Re}\{Y_{Conv}(j\omega)\} = \frac{R_d \cos(\frac{3\pi}{\omega_s}\omega)(1-\omega^2/\omega_{anti}^2)}{A^2 + B^2}$$
$$A = R_d \cos(\frac{3\pi}{\omega_s}\omega) \quad (10)$$
$$B = R_d \sin(\frac{3\pi}{\omega_s}\omega) + \omega(\omega^2 C_f L_{fc} L_{fg} - L_{fc} - L_{fg})$$
$$\omega_s = 2\pi / T_s.$$

Since the denominator is always positive, the only term that specifies the passivity of the admittance is the cosine term which originates from the time delay $G_d(s)$, and the anti-resonance frequency ω_{anti} .

Significant terms of the numerator of (10) are plotted in Fig. 4. The resultant polarity of $\mathrm{Re}\{Y_{Conv}(j\omega)\}$ for three different cases is depicted in Fig. 4 as well, which specifies the passivity zone of the converter output admittance. Polarity of the cosine term changes to negative at ω_{crt} and becomes positive again at the Nyquist frequency ω_N . The other term $(1-\omega^2/\omega_{anti}^2)$ is also plotted for three different cases. Therefore, three different passivity or non-passivity zone can be defined depending on the value of ω_{anti} .

In the case that ω_{anti} is smaller than ω_{crt} , the non-passive zone becomes $(\omega_{anti}, \omega_{crt})$ and when ω_{anti} is larger than ω_{crt} the non-passive zone becomes $(\omega_{crt}, \omega_{anti})$. As a closing remark, when ω_{anti} is equal to ω_{crt} , the non-passive zone vanishes and the harmonic stability would be achieved for all passive network admittances. It should be noted that the frequency range for harmonic stability analysis is confined to the Nyquist frequency ω_N for the straightforward illustration of the interactions between various parameters. Therefore, this paper investigates the harmonic stability of the PSCS-based grid-connected converter with LCL filter over frequencies up to ω_N and presents sufficient constraints to achieve harmonic stability in weak grids with passive admittances.

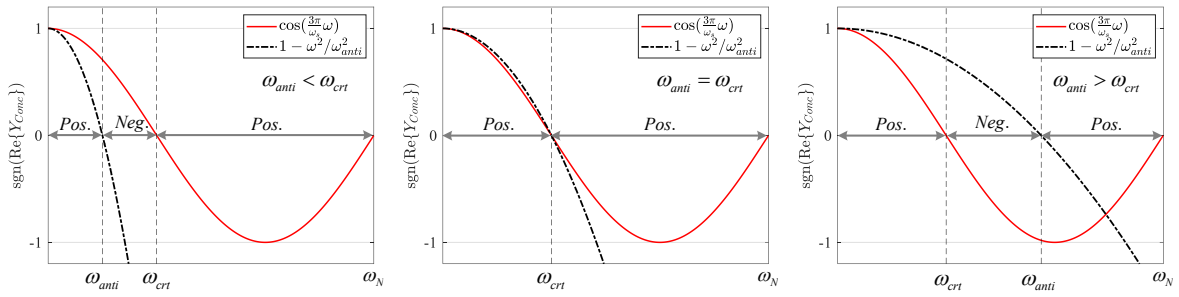

Fig. 4. Sign of $\mathrm{Re}\{Y_{Conv}(j\omega)\}$ and the passivity regions of converter output admittance $Y_{Conv}(s)$.

IV. Harmonic Stability Analysis in Weak Grids for Various Grid Admittances

In this section, harmonic stability analysis of the grid-connected converter system under weak grid operating condition is presented for different grid admittance $Y_{Grid}(s)$. Grid admittance plays an integral role in the harmonic stability of the system. By assuming a passive grid admittance, the interaction of the converter output admittance $Y_{Conv}(s)$ and the grid admittance $Y_{Grid}(s)$ is illustrated in Fig. 5 and modelled in Fig. 6. The non-passive zone of the converter output admittance may cause harmonic instability in certain frequency intervals. Accordingly, the critical grid admittance and the valid operating condition for achieving harmonic stability in the system can be put forward.

Harmonic Stability analysis based on the relation between the admittance characteristics of the converter and the grid reveals that the harmonic stability of the interconnected system can be determined by introducing minor loop gain $L_{Minor}(s)$ as:

$$L_{Minor}(s) = \frac{Y_{Conv}(s)}{Y_{Grid}(s)}. \tag{11}$$

The minor loop gain $L_{Minor}(s)$ (illustrated in Fig. 6) provides essential insights that can be used to specify constraints for parameter selection of the LCL filter and the stable operating condition of the converter.

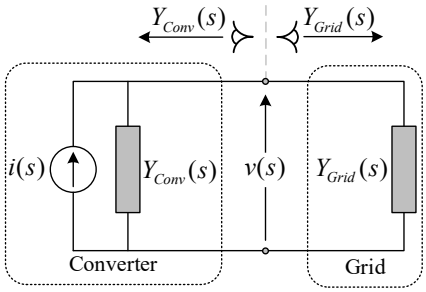

Fig. 5. Admittance representation of a grid-connected converter for harmonic stability analysis.

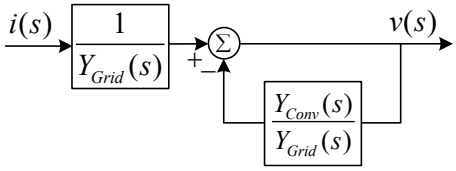

Fig. 6. Demonstration of the admittance minor loop.

The harmonic stability of the system can be realized satisfying two conditions. First the magnitude condition, and second the negative phase angle crossover condition expressed by

$$|Y_{Conv}(j\omega)| > |Y_{Grid}(j\omega)| \tag{12}$$

$$\angle Y_{Conv}(j\omega) - \angle Y_{Grid}(j\omega) = -\pi \pm 2n\pi. \tag{13}$$

Considering an inductive grid admittance, the frequency range of interest is narrowed to the non-passive zone of the converter output admittance. To investigate the magnitude condition for a passive inductive weak grid, the magnitude of the converter output admittance $|Y_{Conv}(j\omega)|$ is plotted in Fig. 7 and Fig. 8 for two different cases where $\omega_{anti} < \omega_{crt}$ and $\omega_{anti} > \omega_{crt}$, respectively. The critical frequency ω_{crt} is where the phase of the converter output admittance $\angle Y_{Conv}(j\omega)$ crosses $\pm\pi/2$. Consequently, the magnitude ratio $|Y_{Conv}(j\omega)|/|Y_{Grid}(j\omega)|$ at ω_{crt} is the preliminary stage in the harmonic stability assessment. In this section, to study the effect of the grid admittance on the harmonic stability of the system, two different short circuit ratios (SCRs) are considered for the grid which represent the strong grid operating condition ($SCR = 15$) and the very weak grid operating condition ($SCR = 1.5$). For a passive inductive grid, the critical inductance value of the grid can be obtained by matching the grid admittance magnitude $|Y_{Grid}(j\omega)|$ to the converter output admittance $|Y_{Conv}(j\omega)|$ at the critical frequency ω_{crt} as:

$$Y_{Grid}(j\omega) = Y_{Conv}(j\omega)\big|_{\omega=\omega_{crt}}. \tag{14}$$

By decreasing the SCR of the grid, the grid admittance line $|Y_{Grid}(j\omega)|$ moves downwards as depicted with dashed lines in Fig. 7 and Fig. 8. As a result, the frequency range of satisfying the magnitude condition $|Y_{Conv}(j\omega)| > |Y_{Grid}(j\omega)|$ widens. Consequently, the frequency in which the negative crossover occurs $(\angle Y_{Conv} - \angle Y_{Grid} = -\pi \pm 2n\pi)$ in this circumstance ω_{crt}, would be encompassed in the magnitude inversion zone as depicted in Fig. 7 and Fig. 8.

However, taking into account the anti-resonance frequency ω_{anti}, the phase difference between the two admittances would be equal to zero at ω_{crt} because of the phase angle of the grid admittance ($-\pi/2$ phase angle). This is the most stable condition which is shown in Fig. 8. In a nutshell, the harmonic stability of the system would be jeopardized in high-impedance weak grid operating condition only when ω_{anti} is smaller than ω_{crt} and the grid inductance L_{Grid} is larger than L_{Grid}^{crt} expressed by

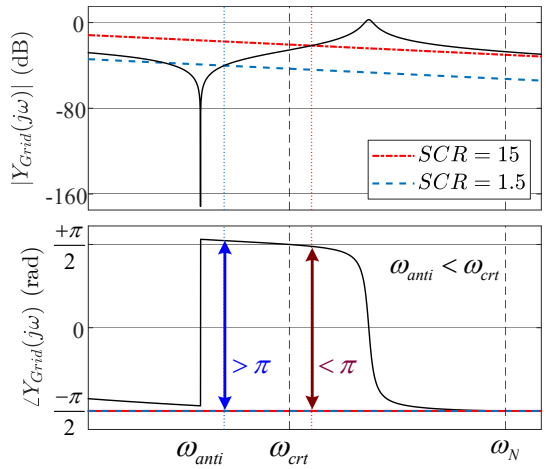

Fig. 7. Harmonic stability assessment of the grid-connected converter system when $\omega_{anti} < \omega_{crt}$ for two different grid SCRs.

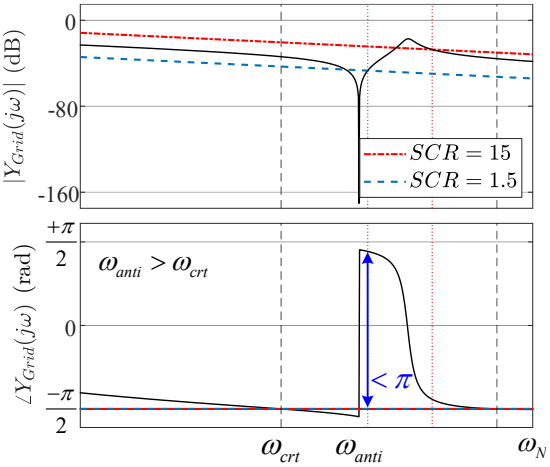

Fig. 8. Harmonic stability assessment of the grid-connected converter system when $\omega_{anti} > \omega_{crt}$ for two different grid SCRs.

$$L_{Grid}^{crt} = \frac{\sqrt{A_{crt}^2 + B_{crt}^2}}{\omega_{crt}\left|1 - \omega_{crt}^2 C_f L_{fc}\right|}$$

$$A_{crt} = R_d \cos(\frac{3\pi}{\omega_s}\omega_{crt}) \qquad (15)$$

$$B_{crt} = R_d \sin(\frac{3\pi}{\omega_s}\omega_{crt}) + \omega_{crt}(\omega_{crt}^2 C_f L_{fc} L_{fg} - L_{fc} - L_{fg}).$$

V. System Description and Simulation Results

To validate the harmonic stability analysis proposed in this paper for weak grid applications, time-domain simulations in MATLAB were carried out. The simulated PSCS-based grid-connected converter, as shown in Fig. 1, is linked to the grid via an LCL filter with passive damping resistors in series with the filter capacitors. The power rating of the converter and the parameters of the LCL filter are given in Table I.

Two case studies are taken to illustrate the influence of the sampling frequency and the LCL filter parameter selection regarding the harmonic stability of the grid-connected converter system under weak grid operating condition. First, the impact of the grid admittance variation on the harmonic stability is presented for the case that the anti-resonance frequency is smaller than the critical frequency $(\omega_{anti} < \omega_{crt})$. Second, the influence of the grid admittance variation for the case that the anti-resonance frequency is greater than the critical frequency $(\omega_{anti} > \omega_{crt})$.

A. Case Study I: $\omega_{anti} < \omega_{crt}$

Simulation results of the PSCS-based grid-connected converter system for the case that the anti-resonance frequency is smaller than the critical frequency $(\omega_{anti} < \omega_{crt})$ is presented in Fig. 9. Time-domain simulations were carried out for both strong grid (SCR=8) and weak grid (SCR=2.5) operating conditions as shown in Fig. 9(a) and Fig. 9(b), respectively. Active power reference of the converter was set to the rated value and an inductive grid admittance was assumed. The parameters of the filter components are summarized in Table I as well. The voltage at the point of common coupling (PCC) and the current of the converter imply that the admittance interaction within the system causes harmonic instability under weak-grid operating condition when $(\omega_{anti} < \omega_{crt})$. It is seen that the harmonic components are oscillating in the grid-connected converter system.

B. Case Study II: $\omega_{anti} > \omega_{crt}$

The PCC voltage and the converter current are depicted in Fig. 10 for the case that the anti-resonance frequency is greater than the critical frequency $(\omega_{anti} > \omega_{crt})$. Similar to the previous case study, the time-domain simulations were carried out for both strong grid (SCR=8) and weak grid (SCR=2.5) operating conditions as shown in Fig. 10(a) and Fig. 10(b), respectively. The parameters of the LCL filter for this case study are summarized in Table I. It is seen that in comparison to the previous case in which $(\omega_{anti} < \omega_{crt})$, the content of the harmonic components in the PCC voltage has reduced considerably and the effect of the grid admittance variation on the harmonic stability of the system is negligible.

In summary, when the anti-resonance frequency is greater than the critical frequency $(\omega_{anti} > \omega_{crt})$, the effect of the grid admittance variation, which is one of the main characteristics of the power-electronics-dominated power systems and the weak-grid operating conditions, would be negligible and the harmonic component oscillations would be damped inherently. Thus, the harmonic stability would be achieved.

TABLE I. Grid-Connected Converter System Specification and Parameters

Parameter	Value
Rated power [kVA]	12.4
Rated current [A]	18
High-pass filter bandwidth ω_b [rad/sec]	60
Active damping resistance R_d [p.u.]	0.2
PSL integral gain K_{ip}	9.343e-3
Sampling frequency [rad/sec]	31416
Critical frequency ω_{crt} [rad/sec]	5236
Case study I $(\omega_{anti} < \omega_{crt})$	
Filter inductance L_{fc} [mH]	6
Filter capacitance C_f [μF]	8
Filter inductance L_{fg} [mH]	2.28
Anti-resonance frequency ω_{anti} [rad/sec]	4564
Case study II $(\omega_{anti} > \omega_{crt})$	
Filter inductance L_{fc} [mH]	4.5
Filter capacitance C_f [μF]	5
Filter inductance L_{fg} [mH]	4.3
Anti-resonance frequency ω_{anti} [rad/sec]	6667

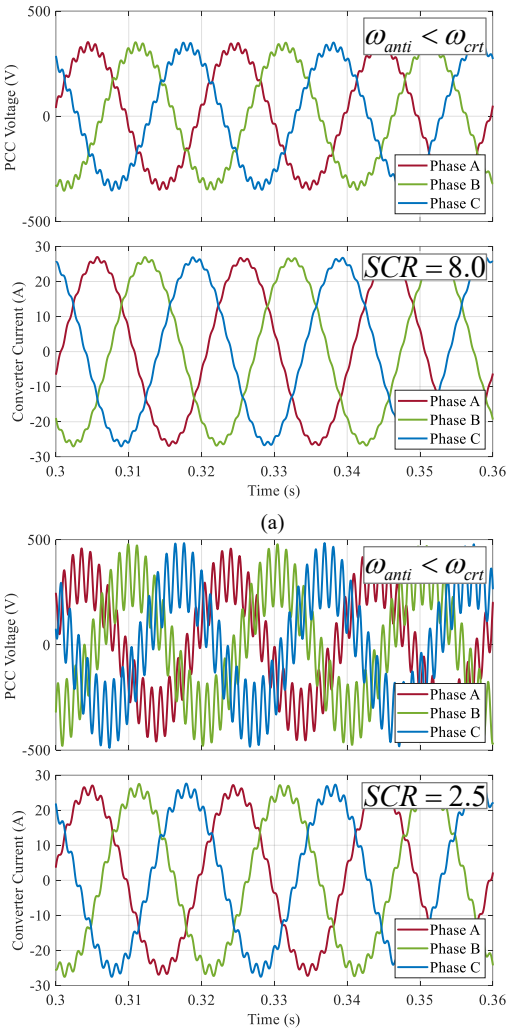

Fig. 9. Time-domain simulation of the grid-connected converter system when $\omega_{anti} < \omega_{crt}$ for two different grid SCRs: (a) SCR=8; (b) SCR=2.5.

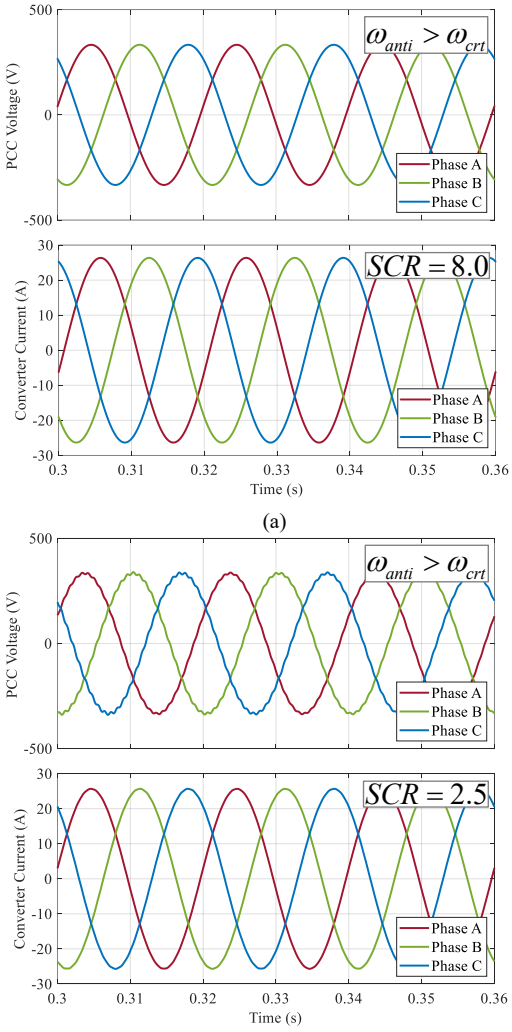

Fig. 10. Time-domain simulation of the grid-connected converter system when $\omega_{anti} > \omega_{crt}$ for two different grid SCRs: (a) SCR=8; (b) SCR=2.5.

This shows a close match between the proposed theoretical analysis and the obtained simulation results.

VI. CONCLUSION

In this paper, the harmonic stability of PSCS-based grid-connected converter systems has been analyzed. Then, it has been revealed that the grid-admittance variation under weak-grid operating condition can jeopardize the harmonic stability of the system. The presented analysis showed that by proper selection of the LCL-filter components regarding the sampling frequency and structure of the control system, it is possible to diminish appropriately the effect of the grid admittance variation on the harmonic stability of the system. In addition, necessary conditions for achieving harmonic stability have been established. Finally, the provided time-domain simulations verified the corresponding analysis and demonstrated the high agreement between the proposed theoretical analysis and the obtained simulation results.

REFERENCES

[1] X. Wang, F. Blaabjerg and W. Wu, "Modeling and Analysis of Harmonic Stability in an AC Power-Electronics-Based Power System," *IEEE Transactions on Power Electronics*, vol. 29, no. 12, pp. 6421-6432, Dec. 2014.

[2] X. Wang and F. Blaabjerg, "Harmonic Stability in Power Electronic-Based Power Systems: Concept, Modeling, and Analysis," *IEEE Transactions on Smart Grid*, vol. 10, no. 3, pp. 2858-2870, May 2019.

[3] A. Sepehr, E. Pouresmaeil, M. Saeedian, M. Routimo, R. Godina and A. Yousefi-Talouki, "Control of Grid-Tied Converters for Integration of Renewable Energy Sources into the Weak Grids," in *2019 International Conference on Smart Energy Systems and Technologies (SEST)*, 2019, pp. 1-6.

[4] C. Yoon, H. Bai, R. N. Beres, X. Wang, C. L. Bak and F. Blaabjerg, "Harmonic Stability Assessment for Multiparalleled, Grid-Connected Inverters," *IEEE Transactions on Sustainable Energy*, vol. 7, no. 4, pp. 1388-1397, Oct. 2016.

[5] A. Sepehr, M. Pouresmaeil, M. Hojabri, F. Blaabjerg, E. Pouresmaeil, "Improving Transient Stability of Power Synchronization Control for Weak Grid Applications," in *2020 IEEE 21st Workshop on Control and Modeling for Power Electronics (COMPEL)*, 2020, pp. 1-6.

[6] L. Harnefors, F. M. M. Rahman, M. Hinkkanen and M. Routimo, "Reference-Feedforward Power-Synchronization Control," *IEEE Transactions on Power Electronics*, vol. 35, no. 9, pp. 8878-8881, Sept. 2020.

[7] K. M. Alawasa and Y. A. I. Mohamed, "Impedance and Damping Characteristics of Grid-Connected VSCs With Power Synchronization Control Strategy," *IEEE Transactions on Power Systems*, vol. 30, no. 2, pp. 952-961, March 2015.

[8] K. M. Alawasa and Y. A. I. Mohamed, "Impedance and Damping Characteristics of Grid-Connected VSCs With Power Synchronization Control Strategy," *IEEE Transactions on Power Systems*, vol. 30, no. 2, pp. 952-961, March 2015.